

# Systematics in the superconducting and normal state properties in chemically substituted $\text{MgB}_2$

S. Jemima Balaselvi, A.Bharathi\*, V.Sankara Sastry, G.L.N.Reddy and Y.Hariharan

*Materials Science Division, Indira Gandhi Center for Atomic Research, Kalpakkam, Tamil Nadu 603 102, INDIA\**

(Dated: February 24, 2003)

The superconducting transition temperature,  $T_C$ , the residual resistivity  $\rho_0$  and the slope of resistivity curve at high temperature,  $d\rho/dT$ , have been measured in a series of  $\text{MgB}_2$  samples that have been chemically substituted to varying degree with Li or Cu at the Mg-site and by Li or Cu at the Mg-site along with C substitution at the B-site. DC resistivity and ac susceptibility measurements were employed to extract the above parameters.  $T_C$  versus the electron count (estimated from simple chemical valence count arguments) shows a universal behaviour, with  $T_C$  being constant at the  $\text{MgB}_2$  value for electron counts lower than in  $\text{MgB}_2$  but rapidly decreasing for larger electron counts. The temperature dependence of resistivity in the normal state fits to the Bloch-Grüneisen formula, from which the Debye temperature,  $\theta_D$ , and the  $\rho_0$  are extracted.  $\theta_D$  variation with  $T_C$  is not systematic, whereas  $\rho_0$  versus  $T_C$  shows a systematic variation that depends on the type of the chemical substituent. This dependence has a signature of the nature of the intraband/interband scattering affected by the chemical substitutions.  $d\rho/dT$  increases with C substitution, but decreases with Li and Cu substitution, implying that C substitution leads to the domination of conductivity by the  $\sigma$  band, while in the Li/Cu substituted samples the  $\pi$  band dominates conduction.

PACS numbers: 74.25.Fy, 74.70.Ad, 74.62.-c, 74.62.Dh

## I. 1. INTRODUCTION

Starting with the discovery of superconductivity at 39K in  $\text{MgB}_2$ <sup>1</sup>, there has been hectic activity both theoretical and experimental to unravel the origin of superconductivity in this system. The reduced isotope effect<sup>2,3</sup> and the negative pressure coefficient<sup>4,5</sup> of  $T_C$  seems to indicate that  $\text{MgB}_2$  falls in the category of conventional electron-phonon coupled superconductors with a large electron phonon coupling constant<sup>2,3</sup>. Detailed band structure calculations performed on the system suggest that the Fermi surface consists of two cylinders arising from hole-like  $\sigma$  bonding bands and one electron like and another hole like 3-dimensional tubular network arising from the bonding and the antibonding  $\pi$  bands.<sup>6,7</sup> The phonon density of states has also been calculated for the system from which it is now clear that the  $E_{2g}$  phonon couples non-linearly with holes in the  $\sigma$  band and that it is also anharmonic.<sup>8,9</sup> The presence of both  $\sigma$  and  $\pi$  bands at the Fermi surface and their different couplings with the phonons result in a k-dependent superconducting gap<sup>10</sup> hitherto not observed in earlier superconductors. An effective two gap superconductivity seems sufficient to describe the anomalous specific heat and tunneling data in  $\text{MgB}_2$ .<sup>11,12</sup> Evidence for multigap superconductivity is now accruing from scanning tunneling microscopy, Raman scattering and point contact spectroscopy.<sup>13,14,15</sup>

Various chemical substitutions have been carried out primarily to increase  $T_C$  and to verify several of the early theoretical predictions. The substituents at Mg site that have been examined are Al,<sup>16,17,18</sup> Si,<sup>19</sup> alkali metals,<sup>20,21,22</sup> 3d transition metals<sup>23,24,25</sup> and 4d transition metals.<sup>26,27</sup> These substitutions have almost always resulted in a decrease in  $T_C$ , irrespective of whether the substituent is an electron dopant or a hole dopant, with the exception of Zn substitution in which an increase in  $T_c$  of  $\sim 0.2\text{K}$  was observed. This increase was found to correlate with an expansion of the lattice.<sup>23,24</sup> A similar correlation of the volume expansion with a  $T_C$  increase was also observed in our previous study on 4d- transition metal substitution in  $\text{MgB}_2$  where a small ( $\sim 0.5\text{K}$ ) increase in  $T_C$  was observed for 5% Nb substitution in  $\text{MgB}_2$ .<sup>27</sup> One of the systems studied in detail has been  $\text{Mg}_{1-x}\text{Al}_x\text{B}_2$ <sup>16</sup> in which  $T_C$  shows a monotonic decrease with substitution in the  $x=0.0$  to  $x=0.3$  composition range, there is an abrupt decrease in  $T_C$  at  $x=0.33$ , beyond which again a monotonic decrease in  $T_C$  is observed<sup>17</sup>. There is also an associated compression along the c-axis and along the a-axis resulting in a net decrease in the cell volume. Thermopower studies in this series showed that the charge carriers are holes and the decrease in  $T_C$  correlates with the decrease in the hole density of states at the Fermi level<sup>18</sup> as a result of electron doping in the system. Band structure calculations carried out in Al substituted  $\text{MgB}_2$  indicates a decrease in the area of the cylindrical part of the Fermi surface with substitution, which also correlates rather well with the decrease in  $T_C$  with Al substitution.<sup>28</sup> Be substitution in  $\text{MgB}_{2-x}\text{Be}_x$ , results in a decrease in a- lattice parameter and in an increase in c- lattice parameter resulting in a net increase in volume, and phase stability in this system was observed upto  $x=0.6$ . Thermopower measurements showed an increase in hole concentration with Be substitution. Thus in the Be substituted samples despite an increase in cell volume and an increase in the hole concentration,  $T_C$  decreases. It is reasoned that the decrease in  $T_C$  is correlated with the decrease in 'a' lattice parameter which leads to a depletion of charge at the B site, causing an increase in phonon frequency and decrease in electron phonon coupling.<sup>29,30</sup> Carbon substitution at B site,<sup>31,32,33,34,35,36</sup> reported by different groups

showed a decrease in  $T_C$  and cell volume with increase in C content. The decrease in  $T_C$  is attributed to a decrease in hole density of states at the Fermi level due to electron doping. The small differences in the extent of decrease in  $T_C$  among the various reports arise on account of the differences of C solubility into the  $\text{MgB}_2$  lattice. This variation in solubility has been attributed to the form of C employed in the synthesis and the method of sample preparation. We have reported<sup>36</sup> a C solubility upto  $x=0.30$  in  $\text{MgB}_{2-x}\text{C}_x$  and a decrease in  $T_C$  of upto  $\sim 26\text{K}$  in these samples, made using a home built 50 bar pressure lock-in set-up. The decrease in  $T_C$  with C concentration matches with that observed for Al substitution, possibly indicating that the additional electrons due to C/Al substitution fill the  $\text{MgB}_2$  bands in a rigid band manner. From the substitution studies, discussed above, it is clear that electron doping results in a decrease in  $T_C$ , and an increase in  $T_C$  due to hole doping has not been observed.

Calculations<sup>37</sup> predicted an increase in  $T_C$  by complete substitution of Mg by Cu and partial C substitution of B in the  $\text{MgB}_2$  lattice. The rationale behind the prediction was that C substitution for B would result in an increase in stiffness of B-C bond and hence the electron-phonon coupling strength. Since C substitution results in electron doping, known to deplete  $T_C$ , it was thought that substitution of Cu for Mg would provide the compensating holes in the system. Search along similar lines led to the prediction of hole doped LiBC to be a high temperature superconductor,<sup>38</sup> in which the presence of the B-C network results in a large electron-phonon interaction.

Early band structure calculations<sup>7</sup> also point out that the hole DOS in  $\text{MgB}_2$  is 2-dimensional in character and that an increase in the hole concentration may not result in an increase in  $T_C$ . It was shown that hole DOS is flat below  $E_F$ , i.e., will remain constant with hole doping but falls off slowly with a small increase in electron doping and rather precipitously beyond 0.2 electron addition per formula unit. In our earlier study on C doped  $\text{MgB}_2$ , we indeed did see a large decrease in  $T_C$  with large electron dopings, which could be attributed to a precipitous decrease in the hole DOS. In an attempt to check the hole DOS picture further, we started out on the synthesis of samples with differing hole concentration levels by suitable Li and Cu substitution and have examined the variation in  $T_C$  in them with electron addition by C substitution. The two initial hole dopings we started out with were 20% Li substituted and 5% Cu substituted  $\text{MgB}_2$ . These compositions were arrived at based on the determination of individual solubilities of Cu and Li in  $\text{MgB}_2$  by systematic chemical substitution studies of Cu and Li respectively.

The different series of samples that are examined in this work are, Li and Cu substitution at Mg site to study the effect of holes viz.,  $\text{Mg}_{1-x}\text{Li}_x\text{B}_2$  and  $\text{Mg}_{1-x}\text{Cu}_x\text{B}_2$  and electron doping by C substitution at B site along with hole doping of 20%Li and 5%Cu at the Mg site, viz.,  $\text{Mg}_{0.80}\text{Li}_{0.20}\text{B}_{2-x}\text{C}_x$  and  $\text{Mg}_{0.95}\text{Cu}_{0.05}\text{B}_{2-x}\text{C}_x$ . The experimental techniques employed in this study are ac susceptibility measurement for determining  $T_C$  and resistivity measurement from 300K to 4.2K, to determine  $T_C$  and normal state transport. The superconducting transition temperatures are extracted from the onset of the diamagnetic signal and from the zero resistance. The temperature dependent normal state resistivity is fitted to the Bloch-Gruneisen formula to extract the Debye temperature  $\theta_D$  and residual resistivity  $\rho_0$ . Using this  $\theta_D$  and the measured  $T_C$  in the McMillan equation, the electron-phonon coupling  $\lambda$  is extracted. The slope of the linear part of the resistivity curve in the 200K-300K temperature range has also been determined in each of the samples, in order to quantify the magnitude of the temperature dependence of resistivity. The various measured parameters on these samples have been compared with that in  $\text{MgB}_{2-x}\text{C}_x$ .<sup>36</sup> The paper is organized as follows. In section.2 the experimental details are mentioned. In section.3 we present the various results along with the corresponding discussions in different subsections. Section.4 provides the summary and conclusions.

## II. 2. EXPERIMENTAL

Samples of nominal composition  $\text{Mg}_{1-x}\text{Li}_x\text{B}_2$  [ $x=0.1, 0.2, 0.3$ ],  $\text{Mg}_{1-x}\text{Cu}_x\text{B}_2$  [ $x=0.01, 0.02, 0.025, 0.05$ ],  $\text{Mg}_{0.80}\text{Li}_{0.20}\text{B}_{2-x}\text{C}_x$  [ $x=0.1, 0.2$ ] and  $\text{Mg}_{0.95}\text{Cu}_{0.05}\text{B}_{2-x}\text{C}_x$  [ $x=0.025, 0.05, 0.15, 0.3$ ] were prepared by the standard solid-vapour technique using Mg powder (99.9%), amorphous boron (99%), carbon soot (99%) obtained from fullerene synthesis, Li pieces (99%) and Cu powder (99.9%). The stoichiometric quantities are weighed, mixed and compacted into a Ta crucible and heat treated at  $900^\circ\text{C}$  for 1hour 30 minutes under a locked-in Ar pressure of 50 bar.<sup>36</sup> Li was loaded inside a dry box under Ar atmosphere. Weight loss was consistently recorded to be less than 1% indicating that the nominal composition is preserved even after the heat treatment in all the samples. Samples so obtained were of  $\sim 30\%$  theoretical density and suitable for resistivity measurements by appropriate slicing. However some samples that were not compacted properly, resulted in porous powders, in which resistivity contacts could not be achieved. The samples were characterized by powder X-ray diffraction in a STOE diffractometer using  $\text{Cu-K}_\alpha$  radiation in the Bragg-Brentano geometry. Susceptibility measurements were done by tracing the diamagnetic signal using an ac mutual inductance technique at a measuring frequency of 941 Hz for which 25 mg of finely powdered samples were used. The resistance measurements were done on  $\sim 1\text{mm}$  thick sliced pieces in the standard four probe geometry using, 42 SWG Cu leads with silver paint as contact glue. The resistivity in each sample was measured in the Van der pauw geometry at room temperature, using which resistivity values at all the temperatures could be determined.

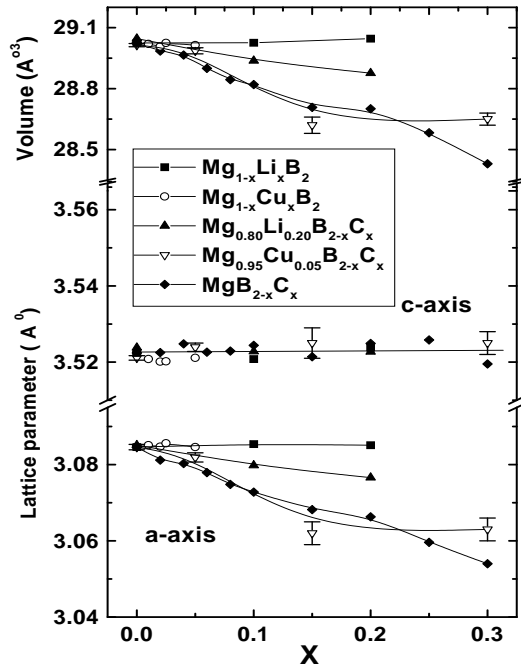


FIG. 1: Plot of the lattice constants 'a' and 'c' and the lattice cell volume, obtained from XRD patterns, as a function of the varying substituent fraction, 'x'. The solid lines are guide to the eye.

For both susceptibility and resistivity measurements, the temperature variation from 300K to 4.2K was obtained by using a dipstick setup in the which the temperature was measured using a Si-diode thermometer with an excitation current of  $10\mu\text{A}$  and the data was collected through a PC, interfaced by IEEE 488 card.

### III. 3. RESULTS AND DISCUSSION

#### A. 3.1 XRD measurements

From the phase purity analysis of the XRD data it is clear that the Li solubility in  $\text{MgB}_2$  is at least 20% ( $x=0.2$ ), while that of Cu is only 5% ( $x=0.05$ ). Carbon substitutes upto a fraction of  $x=0.30$  in a phase pure form in the cation substituted samples. The lattice parameters 'a' and 'c' and the cell volume obtained from an analysis of the XRD data using the STOE program are shown in Fig. 1, as a function of 'x', where x is the fraction of the substituent whose concentration is varied in that particular series. It can be seen from the figure that 'c' parameter remains more or less unchanged with substitution in all the series studied. For cationic substitutions, the 'a' parameter also remains constant, resulting in no change in volume for samples that are substituted only at the Mg site. The lack of change in the lattice parameters with Li substitution in Fig. 1 is at variance with earlier studies<sup>20</sup> where a substantial decrease in 'a' parameter was observed with Li substitution. From Fig. 1, it is seen that with C substitutions the lattice parameter along 'a' decreases monotonically with increasing concentration with a corresponding decrease in the lattice volume. The extent of the decrease is the largest for the  $\text{MgB}_{2-x}\text{C}_x$ , intermediate in  $\text{Mg}_{0.95}\text{Cu}_{0.05}\text{B}_{2-x}\text{C}_x$  and small in  $\text{Mg}_{0.80}\text{Li}_{0.20}\text{B}_{2-x}\text{C}_x$ . The lattice constant remaining unchanged in the Li substituted samples can be rationalized based on the fact that the ionic radii of  $\text{Li}^+$  of  $\text{Mg}^{++}$  are not very different. The lack of change due to Cu substitution can be reconciled with, from the fact that Cu is soluble only to 5% and a difference in the ionic radii may not reflect as a measurable change in lattice constant. The decrease in the a-parameter with C content can result due to the smaller covalent radius of C in comparison with that of B. The smaller decrease in the a-parameter with C substitution in the Li and Cu substituted samples is surprising. The differences in these lattice parameter variations suggest that the electron concentration present in the sample also plays an important role in determining the equilibrium lattice constants.

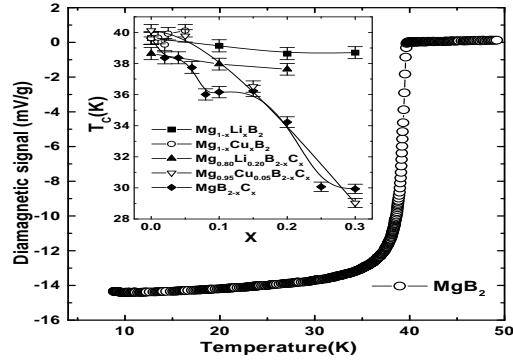


FIG. 2: Plot of diamagnetic signal versus temperature in the range 4.2K-50K for pristine  $\text{MgB}_2$ . In the inset is shown the variation in  $T_C$  with fraction 'x' of varying substituent in the different series studied. The temperature at the 10% signal measured from the onset is taken as  $T_C$ .

TABLE I: Table.1 Data from susceptibility measurements; temperature corresponding to 10% of the total diamagnetic signal, measured from the onset is recorded  $T_C$ ; difference between the temperatures corresponding 10% signal and 90% signal is recorded as  $\Delta T_C$  and the corresponding magnitude of the signal is the volume fraction.

$\text{Mg}_{1-y}\text{M}_y\text{B}_{2-x}\text{C}_x$	M	y	x	$T_c$	$\Delta T_c(\text{K})$	Vol.Frac.(mV/gm)
$\text{MgB}_2$		0	0	39.6	1.75	14.0
$\text{MgB}_{2-x}\text{C}_x$		0	0.02	38.3	2.41	12.9
		0	0.04	38.4	4.13	13.6
		0	0.06	37.7	4.51	13.1
		0	0.08	36.0	4.11	12.8
		0	0.10	36.1	8.08	13.5
		0	0.15	36.2	9.17	11.3
		0	0.20	34.2	14.09	11.5
		0	0.25	30.1	14.66	11.9
		0	0.30	29.9	15.12	9.0
	$\text{Mg}_{1-y}\text{Li}_y\text{B}_2$	Li	0.1	0	39.1	4.5
0.2			0	38.8	4.9	7.6
0.3			0	38.7	5.7	4.9
$\text{Mg}_{0.8}\text{Li}_{0.2}\text{B}_{2-x}\text{C}_x$		0.2	0.1	38.0	3.3	9.6
		0.2	0.2	37.6	5.9	10.1
$\text{Mg}_{1-y}\text{Cu}_y\text{B}_2$	Cu	0.01	0	39.7	3.2	7.1
		0.02	0	39.2	3.5	9.7
		0.025	0	39.9	2.7	8.7
		0.05	0	40.11	2.8	7.7
$\text{Mg}_{0.95}\text{Cu}_{0.05}\text{B}_{2-x}\text{C}_x$		0.05	0.05	39.8	3.4	8.5
		0.05	0.15	36.5	8.8	6.6
		0.05	0.30	29.0	9.5	4.9

### B. 3.2 $T_C$ from ac susceptibility and from dc resistivity

In Fig.2 is shown the variation of the diamagnetic signal for  $\text{MgB}_2$  in the 4.2K to 50K temperature range. The  $T_C$  of 39.6K is deduced by reading off the value of temperature at 10% of the total diamagnetic signal determined from the onset. The transition width ( $\Delta T_C$ ), determined from the difference in temperatures at 90% and 10% of the total diamagnetic signal, was 1.75K. The variation of  $T_C$  along each series is shown in the inset of Fig.2. The observed values of  $T_C$ ,  $\Delta T_C$  and volume fraction of the net diamagnetic signal for the various samples are tabulated in Table.1. [width=8cm,height=8cm]

In Fig.3 is shown the temperature dependence of resistivity curve for pristine  $\text{MgB}_2$ . The value of RR defined as

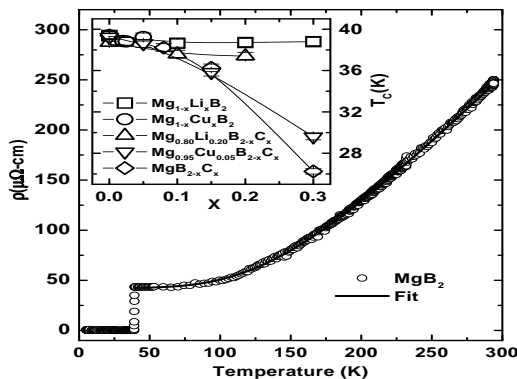


FIG. 3: Fig. 3 Plot of the resistivity versus temperature from 4.2K-300K for pristine MgB<sub>2</sub>. The solid line shows the fitted curve resistivity curve to the Bloch-Gruneisen formula. In the inset is shown the variation in T<sub>C</sub> with the fraction of substituent x for the different series studied. Solid lines in the inset are a guide to the eye.

the ratio of the resistivity at 300K to the resistivity at 40K ( $\rho(300\text{K})/\rho(40\text{K})$ ), observed for MgB<sub>2</sub> was  $\sim 6$  with a T<sub>C</sub> of 39.4K at zero resistance, and the transition width  $\Delta T_C$  determined as the difference in the onset and downset temperature is  $\sim 0.3\text{K}$ . The T<sub>C</sub> variation across the different series, is shown in the inset of Fig.3 and in Table. 2. The variation of T<sub>C</sub> as a function of substituent from the resistivity data is in general agreement with that observed by susceptibility measurements. It is clear from Fig.3 that in the series Mg<sub>1-x</sub>Cu<sub>x</sub>B<sub>2</sub>, T<sub>C</sub> remains almost constant, whereas in Mg<sub>1-x</sub>Li<sub>x</sub>B<sub>2</sub> it shows a small decrease. The transition width is  $\sim 0.3\text{K}$  for all these concentrations. In contrast, in all the carbon substituted samples a systematic decrease in T<sub>C</sub> is seen and the extent of decrease in T<sub>C</sub> is dependent on the amount of cation substituted. Across the series Mg<sub>0.95</sub>Cu<sub>0.05</sub>B<sub>2-x</sub>C<sub>x</sub> a decrease in the T<sub>C</sub> of 10K for a maximum carbon substitution of x=0.3 is observed, compared to a T<sub>C</sub> decrease of 14K in the MgB<sub>2-x</sub>C<sub>x</sub> series for a comparable carbon content. Whereas, in the Mg<sub>0.80</sub>Li<sub>0.20</sub>B<sub>2-x</sub>C<sub>x</sub> series only a decrease of  $\sim 1\text{K}$  is observed and the transition width is also very small of  $\sim 0.5\text{K}$  for all the samples in this particular series. For the other carbon substitutions, as in susceptibility measurements the transition width is seen to increase with the degree of substitution. The differences in the variation of T<sub>C</sub> for a similar extent of carbon substitution, therefore hints at the dependence of T<sub>C</sub> on other factors. We investigate one such possibility below.

### C. 3.4 T<sub>C</sub> versus ρ(electron count)

We define a parameter  $N_{excess}$ , denoting the excess charge (electron/hole) with respect to MgB<sub>2</sub> as

$$N_{excess} = x - y \quad (1)$$

where, x is the fraction of the divalent anion substituent (assumed to donate one electron in excess of MgB<sub>2</sub> for each atom substituted per formula unit) and y is the fraction of monovalent cation (which supplies one extra hole as compared to that in MgB<sub>2</sub> for one atom substituted per formula unit). The general formula for a representative sample studied is given by Mg<sub>1-y</sub>M<sub>y</sub>B<sub>2-x</sub>C<sub>x</sub>, where M=Li or Cu.  $N_{excess}$  can be taken as a qualitative measure of the valence electron concentration, with respect to that in MgB<sub>2</sub>.  $N_{excess}$  is zero for MgB<sub>2</sub>, positive for electron doped MgB<sub>2</sub> and negative for hole doped MgB<sub>2</sub>. A plot of  $N_{excess}$  against T<sub>C</sub> is shown in Fig.4, from which it is clear that the T<sub>C</sub> remains almost constant for  $N_{excess} < 0$  viz., with increase in the hole concentration in MgB<sub>2</sub>, whereas it decreases with increase in electron concentration viz., for  $N_{excess} > 0$ . The prominent feature in Fig.4 is that T<sub>C</sub> variation is the same for all the samples, albeit they belong to different series, depending purely on the electron count in the sample. To illustrate this point, focusing at  $N_{excess}=0$  in Fig.4, obtained from MgB<sub>2</sub>, Mg<sub>0.80</sub>Li<sub>0.20</sub>B<sub>1.80</sub>C<sub>0.20</sub> and Mg<sub>0.95</sub>Cu<sub>0.05</sub>B<sub>1.95</sub>C<sub>0.05</sub>, one sees that the T<sub>C</sub>s are nearly the same. The T<sub>C</sub> versus  $N_{excess}$  plot in Fig.4 holds a striking resemblance to the hole DOS versus energy curve shown by An and Pickett.<sup>7</sup> It was remarked in that paper that T<sub>C</sub> will not increase with hole doping whereas electron doping would result in a decrease in T<sub>C</sub>. From Fig.4

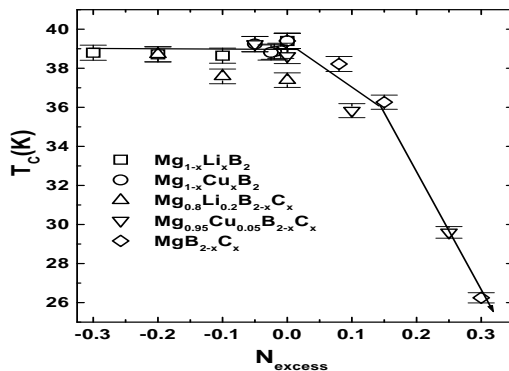


FIG. 4: Plot of  $N_{excess}$  (defined in the text) against  $T_C$  for all the samples. The symbols for the different series are marked in the legend. The solid line is a guide to the eye.

TABLE II: Data from resistivity measurements;  $x$ ,  $y$  and  $N_{excess}$  are described in the text. The temperature corresponding to zero resistivity is shown as  $T_C$ ;  $\theta_D$ ,  $\rho_0$ ,  $\rho_1$  parameters obtained from fitting the normal state resistivity to the Bloch-Gruneisen formula; electron-phonon interaction parameter,  $\lambda$  calculated using McMillan's equation and the slope of  $\rho(T)$  in the 200K-300K range.

$Mg_{1-y}M_yB_{2-x}C_x$	$N_{excess}$ ( $x-y$ )	$T_C$ (K)	$\theta_D$ (K)	$\rho_0$ $\mu\Omega\text{-cm}$	$\rho_1 \times 10^{-3}$ $\mu\Omega\text{-cmK}^{-2}$	$C \times 10^3$ $\mu\Omega\text{-cmK}$	$\lambda$	$d\rho/dT$
$MgB_2$	0	39.4	911.9	41.92	0.2536	3.6761	0.8408	1.2083
$MgB_{1.92}C_{0.08}$	0.08	38.2	823.4	173.76	1.4118	2.4189	0.8784	1.3238
$MgB_{1.70}C_{0.30}$	0.30	26.2	528.8	948.2	3.339	1.2801	0.9123	2.2609
$Mg_{0.90}Li_{0.10}B_2$	-0.10	38.6	992.7	30.079	0.5079	1.9901	0.8015	0.7683
$Mg_{0.80}Li_{0.20}B_2$	-0.20	38.7	920.1	22.651	0.2011	0.9223	0.8335	0.3779
$Mg_{0.80}Li_{0.20}B_{1.90}C_{0.10}$	-0.10	37.6	851.9	99.569	0.2705	1.5426	0.8545	0.6343
$Mg_{0.80}Li_{0.20}B_{1.80}C_{0.20}$	0	37.4	674.4	271.69	1.3174	2.6158	0.9755	1.6238
$Mg_{0.99}Cu_{0.01}B_2$	-0.01	38.9	936.5	20.550	0.2587	1.1867	0.8280	0.4510
$Mg_{0.98}Cu_{0.02}B_2$	-0.02	38.8	963.4	34.245	0.4864	1.8878	0.7594	0.7715
$Mg_{0.975}Cu_{0.025}B_2$	-0.025	38.8	928.7	16.971	0.2625	1.0823	0.8305	0.4480
$Mg_{0.95}Cu_{0.05}B_2$	-0.05	39.2	852.6	27.226	0.2506	1.4668	0.8780	0.6276
$Mg_{0.95}Cu_{0.05}B_{1.95}C_{0.05}$	0	38.6	800.1	43.603	0.3159	1.3653	0.8979	0.6455
$Mg_{0.95}Cu_{0.05}B_{1.85}C_{0.15}$	0.10	35.8	785.9	137.64	0.2789	1.1841	0.8698	0.5686
$Mg_{0.95}Cu_{0.05}B_{1.70}C_{0.30}$	0.25	29.6	851.9	235.43	0.4922	0.8002	0.7594	0.4978

it appears that the  $T_C$  remains fixed with hole doping, whereas it shows a decrease with electron doping, which is smooth upto an electron doping level of  $\sim 0.2$ , beyond which  $T_C$  drops faster in agreement with the calculation.<sup>7</sup>

#### D. 3.5 Analysis of normal state resistivity

The temperature dependence of the normal state resistivity in  $MgB_2$ , suggests the dominance of phonon scattering.<sup>39,40,41</sup> The normal state resistivity for each of the data from the different series investigated could be fitted to the Bloch-Gruneisen formula, in the 40K and 300K range<sup>41</sup> using

$$\rho(T) = \rho_0 + \rho_1 T^2 + C \rho_{ph}(T) \quad (2)$$

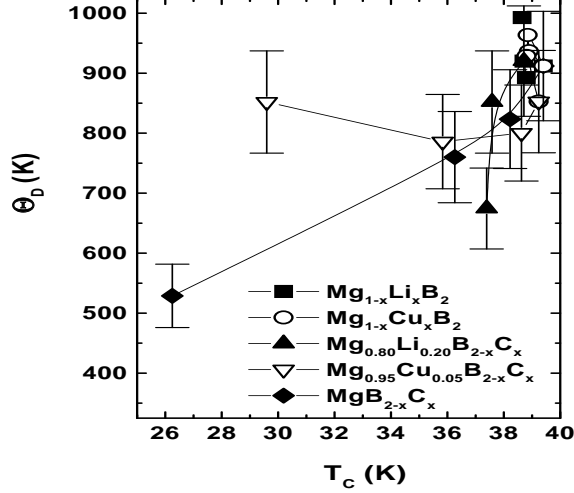


FIG. 5: Plot of  $T_C$  against  $\theta_D$  obtained from the Bloch-Gruneisen fit for all samples studied. Solid lines are guides to the eye.

where  $\rho_{ph}(T)$  is given by

$$\rho_{ph}(T) = (m - 1)\theta_D \left(\frac{T}{\theta_D}\right)^m \int_0^{\frac{\theta_D}{T}} dZ \frac{Z^m}{(1 - e^{-z})(ez - 1)} \quad (3)$$

$\rho_0$  is the impurity scattering contribution to resistivity,  $\rho_1$  denotes the magnitude of the electron-electron interaction parameter,  $m=5$ ,  $\theta_D$  is the Debye temperature and  $C$  is a constant. The fit obtained for  $\text{MgB}_2$ , is shown in Fig.3 along with the experimental data, from which it is apparent that the fit is excellent. A similar quality of fit has been obtained for each of the  $\rho(T)$  data in all the series. From the fit, the value of  $\rho_0$ ,  $\rho_1$ ,  $C$  and  $\theta_D$  were extracted, which are shown in Table 2. The small values of  $\rho_1$  suggest that the contribution from electron-electron scattering to the transport is negligible in the system. The  $\rho_0$  obtained from the Bloch-Gruneisen fits are in close agreement with  $\rho(40\text{K})$ , the measured resistivity prior to the superconducting transition. It can be seen from Table. 2 that  $\theta_D$  decreases with  $C$  substitution, but the extent of the observed decrease is very large in comparison to that expected from mass considerations alone. In the case of  $\text{Li}$  and  $\text{Cu}$  substitutions viz.,  $\text{Mg}_{1-x}\text{M}_x\text{B}_2$  ( $M=\text{Li},\text{Cu}$ ),  $\theta_D$  is seen to remain constant, even though a large increase in  $\theta_D$  in the former and decrease in the latter is expected. Carbon substitution on  $\text{Li}$  substituted samples also shows a similar decrease in  $\theta_D$  as in  $\text{MgB}_{2-x}\text{C}_x$ . But with Carbon substitution, in the 5%  $\text{Cu}$  substituted samples  $\theta_D$  remains constant in contrast to the decrease observed in  $\text{MgB}_{2-x}\text{C}_x$  and  $\text{Mg}_{0.80}\text{Li}_{0.20}\text{B}_{2-x}\text{C}_x$  samples. These  $\theta_D$  variations versus the observed  $T_C$  are shown in Fig.5, from which it is apparent that a systematic does not emerge. It should however be mentioned that the lack of systematics could have its origin on the fact that the Bloch-Gruneisen fits have been made assuming that the conductivity arises from a single dominant band; which is known to be true for pristine  $\text{MgB}_2$ . The good fits to this formula would imply the dominance of single band in the substituted samples also, excepting for the fact that the dominant band could be different as will become apparent from the sections to follow.

From the McMillan equation,

$$T_c = \left(\frac{\theta_D}{1.45}\right) \exp\left[-\frac{1.04(1 + \lambda)}{(\lambda - \mu^*(1 + 0.62\lambda))}\right] \quad (4)$$

using the measured  $T_C$  and the extracted  $\theta_D$ , the electron phonon coupling constant,  $\lambda$  is computed with  $\mu^*=0.15$ . The calculated values (cf. Table 2) for the entire series falls in the range of 0.7 and 1.0, which is in general agreement with values reported from theoretical calculations and specific heat measurements.

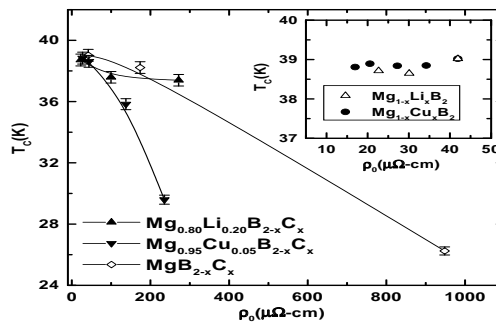


FIG. 6: Plot of  $\rho_0$  versus  $T_C$  where  $\rho_0$  is the residual resistivity obtained from the Bloch-Gruneisen fit of the normal state resistivity data, in all the series studied. Inset shows the data in the Cu and Li substituted samples. The solid lines are a guide to the eye.

### E. 3.6 $\rho_0$ versus $T_C$ correlation

In the  $\text{MgB}_2$  system Matthiesen's rule is violated in that samples that have a large residual resistivity also show a stronger temperature dependence of resistivity.<sup>42</sup> Further, despite the fact that impurity scattering is detrimental to superconductivity in a multiband system,<sup>44</sup>  $T_C$  is robust to the residual resistivity variations in  $\text{MgB}_2$ . These issues have been discussed in a recent calculation<sup>43</sup>, which suggest that the absence of interband scattering between the  $\sigma$  and  $\pi$  bands in  $\text{MgB}_2$  and the dominance intraband  $\sigma$ - $\sigma$  and  $\pi$ - $\pi$  scattering is primarily responsible for this unusual behaviour. It has been shown that the unique electronic structure of  $\text{MgB}_2$  makes  $\sigma$ - $\pi$  hybridization unfavourable, an important pre-requisite for the occurrence of an interband scattering event. Further it has also been demonstrated that by introduction of scattering sites in the Mg sublattice,  $\sigma$ - $\pi$  hybridization is not significantly altered. Calculating the  $T_C$  for different intraband/interband scattering ratios, it has been shown that the slope of the plot of  $\rho_0$  versus  $T_C$  which is negligible for large intraband scattering cross section increases progressively with increase in interband scattering. These results have been compared with the experimental  $T_C$  values that have been obtained for pristine  $\text{MgB}_2$  from different laboratories.

Since in our present study the  $T_C$  and the resistivity behaviour has been examined for a variety of chemical substitutions at the Mg-site, B-site and both Mg and B sites, it appears appropriate to see if any systematics in the variation of  $\rho_0$  with  $T_C$  can be discerned from our data. In Fig.6 is shown the plot of  $\rho_0$  versus  $T_C$  for the different series examined in this work. From Fig.6 it is clear that there is a systematic variation of  $T_C$  with  $\rho_0$  within each series. In the inset of Fig.6 is shown the variation of  $T_C$  with  $\rho_0$  by monovalent cation substitution, which appears almost flat. Taking the cue from calculations<sup>43</sup>, these results suggest that the electronic conduction in the cation substituted samples is dominated by intraband scattering.<sup>43</sup> In the C substituted series the variation of  $T_C$  with  $\rho_0$  is much larger for similar extents of substitution. For example in  $\text{Mg}_{0.95}\text{Cu}_{0.05}\text{B}_{2-x}\text{C}_x$ , the fall of  $T_C$  with  $\rho_0$  is largest, followed by that in  $\text{MgB}_{2-x}\text{C}_x$ , and it is smallest for the Li substituted system viz.,  $\text{Mg}_{0.80}\text{Li}_{0.20}\text{B}_{2-x}\text{C}_x$ . Comparing this with the calculated variation of  $T_C$  with  $\rho_0$ ,<sup>43</sup> clearly suggests that the interband scattering starts playing a role in determining  $\rho_0$  in the carbon substituted samples. This increase in interband scattering could arise from the presence of an excess  $p_z$  electron at the C in the B layer, resulting in the an enhanced  $\sigma$ -  $\pi$  hybridization. This hybridization may get further accentuated in the Cu substituted samples due to the presence of 3d orbitals of Cu, leading to an increased interband scattering and consequently in the pronounced variation of  $\rho_0$  with  $T_C$  in these samples (cf. Fig. 6).

### F. 3.7 Slope of high temperature resistivity

In order to obtain a quantitative measure of the temperature dependence of resistivity in the various samples, the magnitude of  $d\rho/dT$  from the linear regime of  $\rho(T)$  can be extracted. In Fig.7a and Fig.7b are shown the  $\rho(T)$  data

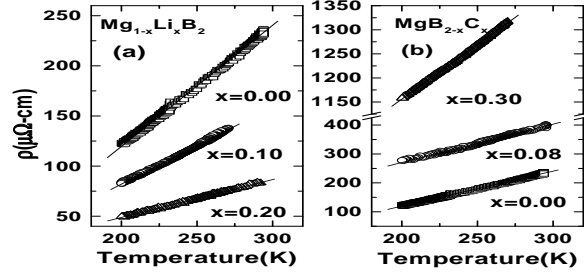


FIG. 7:  $\rho(T)$  in the 200-300K range (a) in  $\text{Mg}_{1-x}\text{Li}_x\text{B}_2$  and in (b)  $\text{MgB}_{2-x}\text{C}_x$ , the solid lines are the linear fits to the data.

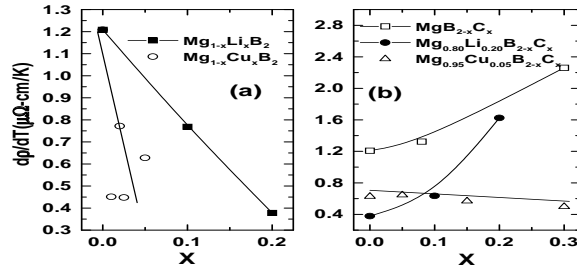


FIG. 8: A plot of  $d\rho/dT$  versus the fraction substituted, for (a) cation substituted samples and (b) for carbon substituted samples. The solid lines are a guide to the eye.

in the 200K-300K temperature range for two representative series viz.,  $\text{Mg}_{1-x}\text{Li}_x\text{B}_2$  and  $\text{MgB}_{2-x}\text{C}_x$ . It is clear from the Figure that in the Li substituted samples the slope decreases, while in the C substituted samples the  $d\rho/dT$  increases with substitution. Similarly the slopes are obtained from a linear fit of the  $\rho(T)$  data in all the samples and are tabulated in Table.2, and also shown in two panels for the cation substituted samples and carbon substitutions in Fig.8a and Fig.8b respectively. A feature that clearly emerges from the data is that the slope decreases by a large extent due to Mg substitution, implying the temperature dependence of  $\rho(T)$  decreases in these samples with substitution. In contrast, in the carbon substituted samples i.e., in  $\text{MgB}_{2-x}\text{C}_x$  and in  $\text{Mg}_{0.80}\text{Li}_{0.20}\text{B}_{2-x}\text{C}_x$  the slope increases with the level of C substituted (cf. Fig. 8b), indicating that the temperature dependence of  $\rho(T)$  increases with substitution. The degree of increase in  $d\rho/dT$  is also high in both the series. In the  $\text{Mg}_{0.95}\text{Cu}_{0.05}\text{B}_{2-x}\text{C}_x$  series, however,  $d\rho/dT$  shows a small decrease. Plotted in Fig.9a and Fig.9b in two panels is the variation of  $\rho_0$  in the different series with substitution. The variation in  $d\rho/dT$  and  $\rho_0$  with the concentration of the substituent are very similar excepting in the  $\text{Mg}_{0.95}\text{Cu}_{0.05}\text{B}_{2-x}\text{C}_x$  series.

In order to obtain a qualitative understanding of the variation in  $\rho_0$  and  $d\rho/dT$  in the various series we take recourse to an analysis of the conductivity in terms of the two band model thought to be most appropriate to understand

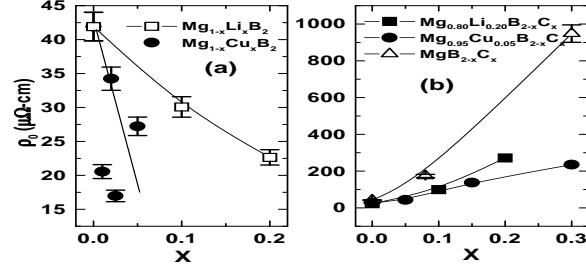


FIG. 9: A plot of  $\rho_0$  versus the substituted fraction in the different series, (a) cation substituted samples (b) carbon substituted samples. The solid lines are a guide to the eye.

normal state transport in  $\text{MgB}_2$ .<sup>43</sup> The expression for conductivity in a two band model<sup>43</sup> is given by

$$\frac{1}{\rho(T)} = \frac{1}{4\pi} \sum_{n=\sigma,\pi} \frac{\omega_{pl,n}^2}{W_n(0,T)}, \quad (5)$$

where  $\omega_{pl,n}$  is the plasma frequency for the band 'n' and  $W_n(0,T)$  for  $n=\sigma$  band is given by

$$W_\sigma(0,T) = \gamma_\sigma + \frac{\pi}{T} \int_0^\infty d\omega \frac{\omega}{\sinh^2(\frac{\omega}{2T})} [\alpha_{tr}^2(\omega) F_{\sigma\sigma}(\omega) + \alpha_{tr}^2(\omega) F_{\sigma\pi}(\omega)] \quad (6)$$

where  $\gamma_\sigma = \gamma_{\sigma\sigma} + \gamma_{\sigma\pi}$ , and  $\gamma_{nn'}$  is the transition probability for an electron to scatter from band index n to n' and  $\alpha_{tr}^2(\omega) F_{nn'}(\omega)$  are the transport Eliashberg functions. The expression  $W_\pi(0,T)$  can be obtained by substituting  $\pi$  for  $\sigma$  in Eq. (6). It is clear from the Eq. (5) that if the  $\sigma$  band i.e; if the first term in Eq. (5) dominates, the temperature dependence of conductivity will be large, since this band is known to couple strongly with phonons in  $\text{MgB}_2$ . On the other hand if the  $\pi$  band dominates conduction, the temperature dependence of conductivity will be small as the  $\pi$  band couples less effectively with phonons in this system. The reduced  $d\rho/dT$  in the cation substituted samples(cf. Fig.8a) and the enhanced  $d\rho/dT$  in the C substituted samples (cf. Fig. 8b) therefore imply that the  $\pi$  band dominates conduction in the former and the  $\sigma$  band dominates conduction in the latter.

The domination of the  $\sigma$  band in the carbon substituted samples ( $\text{MgB}_{2-x}\text{C}_x$  and  $\text{Mg}_{0.80}\text{Li}_{0.20}\text{B}_{2-x}\text{C}_x$ ) would be possible if either the plasma frequency for that band is large or if the  $\gamma_{\pi\pi}$  is large in Eq.5. Since it has been inferred from band structure calculations that the  $\omega_{pl,\sigma}$ <sup>42,43</sup> is small in  $\text{MgB}_2$ , it appears that  $\gamma_{\pi\pi}$  is large in the C substituted samples. This increase in the  $\pi-\pi$  scattering, could arise due to the presence of disorder along the C-axis as a result of the proximity of the  $p_z$  electrons of carbon to this region. The increase in the  $d\rho/dT$  with increase in C content would naturally follow due to the progressive increase in  $\gamma_{\pi\pi}$  consequent to an increase in the number of such scattering centres. The increase in  $\rho_0$  with C substitution which is clearly seen from panels showing the C substitutions in Fig. 9b could arise due to increase in  $\gamma_{\sigma\pi}$ , which is also apparent from Fig.6. In the  $\text{Mg}_{0.95}\text{Cu}_{0.05}\text{B}_{2-x}\text{C}_x$  series the interband scattering term  $\gamma_{\sigma\pi}$  is very large (cf. Fig.6). This could make both the  $\sigma$  and  $\pi$  channels of conduction in Eq.5 equally probable, because of which drawing inferences about the behaviour of either  $\rho_0$  or  $d\rho/dT$  becomes difficult.

The behaviour of  $d\rho/dT$  in the cation substituted samples shows that despite substitution in Mg sublattice the observed temperature dependence of  $\rho(T)$  is smaller than in  $\text{MgB}_2$ , contrary to the findings of the theoretical calculations<sup>43</sup> which indicate that the  $\gamma_{\pi\pi}$  would be large, leading to the domination of the conductivity by the  $\sigma$  band. However the larger contribution to conductivity from the  $\pi$  band (term2 Eq.5), observed in the cation substituted samples (cf. Fig. 8a) could occur if the relative magnitudes of the plasma frequencies from the  $\sigma$  and  $\pi$  bands get strongly affected due to these substitutions. This is highly plausible as it has been demonstrated from band structure calculations of  $\text{LiB}_2$ <sup>42</sup> that the band disposition and dispersion are strongly altered with respect to that in

MgB<sub>2</sub>. It can be seen from Fig. 9a that  $\rho_0$  decreases with substitution in the cation substituted samples, a result rather surprising. These would imply that the intraband  $\pi - \pi$  scattering is progressively reduced due to these substitutions. Band structure calculations would be necessary to verify these experimental observations. Measurements of the normal state resistivity in the Mg<sub>1-x</sub>Al<sub>x</sub>B<sub>2</sub> in which detailed band structure calculations exist are in progress.

#### IV. 4. SUMMARY AND CONCLUSION

The variation of  $T_C$  has been studied as a function of the variation in electron and/or hole concentration by appropriate chemical substitutions. A plot of  $T_C$  versus the electron count estimated from the different series studied shows a universal behaviour, remaining flat for electron counts lesser than the MgB<sub>2</sub> value whereas it steeply decreases with electron count in excess of that in MgB<sub>2</sub>. This has a striking similarity with the variation of hole DOS with energy. The ratio of the interband/intraband scattering seems to be strongly affected by the nature of the chemical dopant. The addition of C to the Boron layer seems to increase  $\gamma_{\sigma\pi}$  resulting in an increase in the residual resistivity and to the depletion of  $T_C$ , which gets further enhanced due to Cu substitution in the Mg sub-lattice. The slope of the resistivity curve in the 200K-300K, gives an indication of the magnitude of the temperature dependence. The larger temperature dependence in the C substituted samples indicates that the  $\sigma$ -band dominates conduction in this system. The temperature dependence of resistivity in the monovalent cation substituted samples are lowered with respect to that in MgB<sub>2</sub>, suggesting an enhanced participation in conductivity due to the  $\pi$ -bands. These results clearly demonstrate that by selective chemical substitutions conductivity from certain bands can be probed.

- 
- \* E-mail: bharathi@igcar.ernet.in
- <sup>1</sup> Jun Nagamatsu, Norimasa Nakagawa, Takahiro Muranaka, Yuji Zenitani, Jun Akimitsu, Nature 410, 63 (2001)
  - <sup>2</sup> S.L.Bud'ko, G.Lapertot, C.Petrovic, C.E.Cunningham, N.Anderson and P.C.Canfield Phys. Rev. Lett. 86, 1877 (2001)
  - <sup>3</sup> D.G.Hinks, H.Claus, J.D.Jorgensen, Nature 411, 457 (2001)
  - <sup>4</sup> B.Lorentz, R.L.Meng, C.W.Chu, cond-mat/0102264
  - <sup>5</sup> T.Tomita, J.J.Hamlin, J.S.Schilling, D.G.Hinks, J.D.Jorgensen, Phys. Rev. B 64, 092505 (2001)
  - <sup>6</sup> J.Kortus, I.I.Mazin, K.D.Belashchenko, V.P.Antropov, L.L.Boyer Phys. Rev. Lett. 86, 4656 (2001)
  - <sup>7</sup> J.M.An, W.E.Pickett, Phys. Rev. Lett. 86, 4366 (2001)
  - <sup>8</sup> T.Yildirim, O.Gulseren, J.W.Lynn, C.M.Brown, T.J.Udovic, Q.Huang, N.Rogado, K.A.Regan, M.A.Hayward, J.S.Slusky, T.He, M.K.Haas, P.Khalifah, K.Inumaru, R.J.Cava, Phys. Rev. Lett. 87, 37001 (2001)
  - <sup>9</sup> Y.Kong, O.V.Dolgov, O.Jepsen, O.K.Andersen, Phys. Rev. B 64, 020501R (2001)
  - <sup>10</sup> Amy.Y.Liu, I.I.Mazin, Jens Kortus, Phys. Rev. Lett. 87, 087005 (2001)
  - <sup>11</sup> F.Bouquet, R.A.Fisher, N.E.Philips, D.G.Hinks, J.D.Jorgensen, Phys. Rev. Lett. 87, 047001 (2001)
  - <sup>12</sup> F.Giubileo, D.Roditchev, W.Sacks, R.Lamy, D.X.Thanh, J.Klein, S.Miraglia, D.Fruchart, J.Marcus, Ph.Monod, Phys. Rev. Lett. 87, 177008 (2001)
  - <sup>13</sup> M. Iavarone, G. Karapetrov, A.E. Koshelev, W. K. Kwok, G. W. Crabtree and D. G. Hinks, Phys. Rev. Lett. **89** 187002 (2002)
  - <sup>14</sup> H. Schmidt, J. F. Zasadzinski, K. E. Gray and D. G. Hinks, Phys. Rev. Lett. **88**, 127002 (2001)
  - <sup>15</sup> X. H. Chen, M. J. Konstantinovic, J. C. Irwin, D. D. Lawrie and J. P. Franck, Phys. Rev. Lett. **87** 157002 (2001)
  - <sup>16</sup> J.S.Slusky, N.Rogado, K.A.Regan, M.A.Hayward, P.Khalifah, T.He, K.Inumani, S.M.Loureiro, M.K.Haas, H.W.Zanderbergen, R.J.Cava, Nature 410, 343 (2001)
  - <sup>17</sup> P.Postorino, A. Congeduti, P. Dore, A. Nucara, A.Bianconi, D. Di Castro, S. De Negri and A. Saccone, Phys. Rev. B **65** 020507(R) (2001)
  - <sup>18</sup> B.Lorentz, R.L.Meng, Y.Y.Xue, C.W.Chu, Phys. Rev. B 64, 052513 (2001)
  - <sup>19</sup> M.R.Cimberle, M.Novak, P.Manfrinetti and A.Palenzona, Supercond. Sci. Technol. 15, 43-47 (2002)
  - <sup>20</sup> Y.G.Zhao, X.P.Zhang, P.T.Qiao, H.T.Zhang, S.L.Jia, B.S.Cao, M.H.Zhu, Z.H.Han, X.L.Wang, B.L.Gu, Physica C 361, 91-94 (2001)
  - <sup>21</sup> S.Y.Li, Y.M.Xiong, W.Q.Mo, R.Fan, C.H.Wang, X.G.Luo, Z.Sun, X.T.Zhang, L.Li, L.Z.Cao, X.H.Chen, Physica C 363, 219-223 (2001)
  - <sup>22</sup> P.Toulemonde, N.Musolino, H.L.Suo, R.Flukiger, cond-mat/0207033 Superconductivity Science and Technology 17-19, (2002)
  - <sup>23</sup> Y.Moritomo, Sh.Xu, cond-mat/0104568
  - <sup>24</sup> S.M.Kazakov, M.Angst, J.Karpinski, I.M.Fita, R.Puzniak, cond-mat/0103350
  - <sup>25</sup> Sheng Xu, Yutaka Moritomo, Kenichi Kato, Arao Nakamura, cond-mat/0104534
  - <sup>26</sup> Vitaly A.Gasparov, N.S.Sidorov, I.I.Zver'kova, M.P.Kulakov, cond-mat/0104323 JETP Letters, April 12 (2001)
  - <sup>27</sup> S.Kalavathi, A.Bharathi, S.Jemima Balaselvi, G.L.N.Reddy, V.S.Sastry, Y.Hariharan, T.S.Radhakrishnan, Solid State Physics (India) 44 (2001)

- <sup>28</sup> O. dela Pena, A. Aguayo and R. des Coss Phys. Rev. B **66** 012511 (2002)
- <sup>29</sup> J.S.Ahn, Young-Jin Kim, M.-S.Kim, S.-I.Lee, E.J.Choi, cond-mat/0202415
- <sup>30</sup> J.S.Ahn, E.S.Choi, W.Kang, D.J.Singh, E.J.Choi, cond-mat/0202457
- <sup>31</sup> Shao-ying Zhang, Jian Zhang, Tong-yum Zhao, Chuan-bing Rong, Bao-gen Shen, Zhao-hua Cheng, cond-mat/0103203
- <sup>32</sup> M.Paranthaman, J.R.Thompson, D.K.Christen, cond-mat/0104086
- <sup>33</sup> Jai Seok Ahn, Eun Jip Choi, cond-mat/0103169
- <sup>34</sup> W.Mickelson, John Cumings, W.Q.Han, A.Zettl, Phys. Rev. B **65**, 052505 (2002)
- <sup>35</sup> T.Takenobu, T.Ito, Dam.H.Chi, K.Prassides, Y.Iwasa, cond-mat/0103241
- <sup>36</sup> A.Bharathi, S.Jemima Balaselvi, S.Kalavathi, G.L.N.Reddy, V.Sankara Sastry, Y.Hariharan, T.S.Radhakrishnan, Physica C **370**, 211-218 (2002)
- <sup>37</sup> M.J.Mehl, D.A.Papaconstantopoulos, D.J.Singh, Phys. Rev. B **64**, 140509R (2001)
- <sup>38</sup> H.Rosner, A.Kitaigorodsky, W.E.Pickett, Phys. Rev. Lett. **88**, 127001 (2002)
- <sup>39</sup> D.K.Finnemore, J.E.Ostenson, S.L.Bud'ko, G.Lapertot, P.C.Canfield, Phys. Rev. Lett. **86**, 2420 (2001)
- <sup>40</sup> P.C.Canfield, D.K.Finnemore, S.L.Bud'ko, J.E.Ostenson, G.Lapertot, C.E.Cunningham, C.Petrovic, Phys. Rev. Lett. **86**, 2423 (2001)
- <sup>41</sup> M.Putti, E.Galleani d'Agliano, D.Marre.F.Napoli, M.Tassisto, P.Manfrinetti, A.Palenzona, C.Rizzato, S.Massidda, Eur. Phys. J. B, **25**, 439-443 (2002)
- <sup>42</sup> I. I. Mazin and V. P. Antropov, Physica C **385**, 49 (2003)
- <sup>43</sup> I.I.Mazin, O.K.Andersen, O.Jepsen, O.V.Dolgov, J.Kortus, A.A.Golubov, A.B.Kuz'menko, D.van der Marel, Phys. Rev. Lett. **89**, 107002 (2002)
- <sup>44</sup> A.A. Golubov and I. I. Mazin, Phys. Rev. B **55** 15146 (1997)